

**LABORATORY EVALUATION OF HMA MIXES MANUFACTURED WITH  
PG64-28NV AND PG64-28PM POLYMER-MODIFIED ASPHALT BINDERS**

**WASHOE REGIONAL TRANSPORTATION COMMISSION  
1105 Terminal Way  
Suite 108  
Reno, NV 89502**

**Final Report  
January 2011**

**UNIVERSITY  
OF NEVADA  
RENO**

---

**Pavements/Materials Program**

**Department of Civil and  
Environmental Engineering  
College of Engineering  
University of Nevada  
Reno, Nevada 89557**

**LABORATORY EVALUATION OF PG64-28PM POLYMER-MODIFIED  
ASPHALT BINDERS**

Authors:

Elie Y. Hajj, Ph.D.

Peter E. Sebaaly, Ph.D., P.E.

Roger Schlierkamp

And

Edward Cortez

Pavements/Materials Program  
Department of Civil & Environmental Engineering  
University of Nevada  
Reno, Nevada 89557

January 2011



## TABLE OF CONTENT

<b>LIST OF TABLES</b> .....	ii
<b>LIST OF FIGURES</b> .....	iii
1. INTRODUCTION .....	1
2. OBJECTIVE .....	1
3. MATERIALS AND MIX DESIGNS .....	2
3.1 Aggregates .....	2
3.2 Asphalt Binders.....	4
3.3 Mix Designs.....	5
4. EXPERIMENTAL PROGRAM.....	9
5. DESCRIPTION OF LABORATORY TESTS .....	10
5.1 Moisture Damage Testing.....	10
5.2 Permanent Deformation Testing.....	12
5.3 Fatigue Cracking Testing.....	13
5.4 Thermal Cracking Testing .....	14
6. ANALYSIS OF LABORATORY TEST RESULTS .....	15
6.1 Resistance of the HMA Mixtures to Moisture Damage.....	15
6.2 Resistance to Permanent Deformation.....	18
6.3 Resistance of the HMA Mixtures to Fatigue .....	20
6.4 Resistance of the HMA Mixtures to Thermal Cracking.....	21
7.0 MECHANISTIC-EMPIRICAL ANALYSIS.....	22
8. CONCLUSIONS.....	24
9.0 REFERENCES .....	27

## LIST OF TABLES

Table 1. Properties of the Aggregate Blend.....	2
Table 2. Gradation of the Aggregate Blend.....	3
Table 3. Asphalt Binders Grading Test Results and Specifications. ....	4
Table 4. Binders PG Grading.....	4
Table 5. Mix Designs Summary and Specifications.....	9
Table 6. Experimental Program.....	10
Table 7. Permanent Deformation Models at 136°F.....	20
Table 8. Fatigue Models at 70°F.....	20
Table 9. Dynamic Modulus of Various Mixes at 10Hz.....	23
Table 10. Results of the Mechanistic-Empirical Analysis.....	24

## LIST OF FIGURES

Figure 1. Gradation of the aggregate blend .....	3
Figure 2. Marshall mix design relationships for PM-PAR .....	6
Figure 3. Marshall mix design relationships for PM-VAL.....	7
Figure 4. Marshall mix design relationships for NV-PAR .....	8
Figure 5. Tensile strength values and ratios at 77°F .....	9
Figure 6. Components of the dynamic modulus test and typical E* master curve.....	11
Figure 7. Components of repeated load triaxial test and typical permanent deformation curve ..	12
Figure 8. Components of beam fatigue test and typical fatigue curve at a given temperature.....	14
Figure 9. Components of TSRST test and typical stress-temperature curves for HMA mixes ....	15
Figure 10. E* at multiple F-T cycles for the Paramount PG64-28PM mixture (PM-PAR) .....	16
Figure 11. E* at multiple F-T cycles for the Valero PG64-28PM mixture (PM-VAL) .....	16
Figure 12. E* at multiple F-T cycles for the Paramount PG64-28NV mixture (NV-PAR) .....	17
Figure 13. Dynamic Modulus E* at 10 Hz and 70°F as a function of freeze-thaw cycles.....	17
Figure 14. Dynamic Modulus Ratio of the various mixtures at 1 and 6 F-T cycles.....	18
Figure 15. Flow number test results at 136°F for the various mixtures.....	19
Figure 16. Permanent deformation at 136°F for the various mixtures .....	19
Figure 17. Flexural beam fatigue relationships at 70°F for the various HMA mixes.....	21
Figure 18. Thermal cracking characteristics of the various mixtures.....	21
Figure 19. Comparison of the variations in the behavior of NV and PM mixtures (a) RLT at 58°C and (b) flexural beam fatigue at 70°F .....	26

## **1. INTRODUCTION**

As part of the implementation of the Superpave performance grade (PG) system, several state highway agencies that experienced good performance with polymer-modified hot mix asphalt (HMA) mixtures have created the PG “plus” specifications to ensure the inclusion of polymers in the asphalt binders. The Nevada Department of Transportation (NDOT) specifies the use of PG64-28NV polymer-modified asphalt binders with all mixtures to be placed on roadways under its jurisdiction in the northern part of the state. The “NV” extension indicates that the binder meet the NDOT PG “plus” specifications which includes the standard Superpave PG binder system plus the following properties: toughness and tenacity on original binder at 77°F and ductility on original and RTFO binder at 40°F. Historical data showed that polymer-modified asphalt binders that meet the NDOT PG “plus” specifications resulted in mixtures with outstanding performance in Nevada.

On the other hand, the California Department of Transportation (CalTrans) specifies the use of PG64-28PM polymer-modified asphalt binders with their dense-graded asphalt mixtures in some parts of the state. The “PM” extension indicates that the binder meet the CalTrans PG “plus” specifications which includes the standard Superpave PG binder system plus the following properties: maximum phase angle on RTFO binder at the high critical performance temperature and elastic recovery on RTFO binder at 77°F.

Currently, the Washoe Regional Transportation Commission (RTC) recommends the use of PG64-28NV polymer-modified asphalt binders in their HMA mixtures. Recently, paving contractors have approached RTC with the request to authorize the use of PG64-28PM in place of the PG64-28NV asphalt binder. Recognizing the good performance of PG64-28NV mixtures and the limited experience with PG64-28PM mixtures in northern Nevada, the RTC sponsored this research study to assess and contrast the performance of HMA mixes manufactured with PG64-28PM to those produced with PG64-28NV. The experimental plan included two sources for the asphalt binders along with a single source of aggregate. A total of four HMA mixes were anticipated in this study: two mixes with PG64-28PM and two mixes with PG64-28NV. All mix designs were conducted at the University of Nevada laboratory and were done in accordance with the Standard Specifications for Public Works Construction (SSPWC) and The Asphalt Institute MS-2 for Marshall mix design method. The aggregate gradation was designed to meet RTC Type 2 specification. A series of tests were conducted to evaluate the resistance of the various mixtures to moisture damage, permanent deformation, fatigue cracking and low temperature thermal cracking.

## **2. OBJECTIVE**

The purpose of this study was to evaluate and compare the mechanical properties of asphalt mixtures manufactured with PG64-28PM to those manufactured with PG64-28NV. Additionally, a mechanistic-empirical analysis was conducted to evaluate the impact of the two polymer-modified HMA mixtures on predicted pavement performance.

### 3. MATERIALS AND MIX DESIGNS

#### 3.1 Aggregates

All mix designs were conducted using the aggregate source located in Mustang, Nevada, owned by the Sierra Nevada Construction (SNC). The mix design used five stockpiles: 3/4", 1/2", 3/8", Crushed Fines and Washed Sand. Hydrated lime was added to the mix at a rate of 1.5% by dry weight of aggregate and marinated for 48 hours. The gradation of the blend aggregate met the Standard Specifications for Public Works Construction, SSPWC, (Orange Book, 2007) for Type 2 gradation. The blend for mix design was as follows:

3/4" Stockpile: 10%  
1/2" Stockpile: 25%  
3/8" Stockpile: 13%  
Crushed Fines: 42%  
Washed Sand: 10%

The following properties were measured on the aggregate blend:

Specific gravity and absorption of coarse aggregate  
Specific gravity and absorption of fine aggregate

In addition to the blend properties, the following properties were collected from the Sierra Nevada Construction Company:

Fractured faces (coarse fraction): one face and two faces  
Liquid limit of combined grading  
Plasticity Index if combined grading  
Percentage of wear  
Soundness, coarse aggregate  
Soundness, fine aggregate

Table 1 summarizes the properties of the aggregate blend. Table 1 and Figure 1 show the gradation of the blend.

Table 1. Properties of the Aggregate Blend.

Property	Values
Absorption, Coarse Aggregate	1.89
Absorption, Fine Aggregate	2.91
Bulk Specific Gravity (Dry), Coarse Aggregate	2.68
Bulk Specific Gravity (Dry), Fine Aggregate	2.61

Table 2. Gradation of the Aggregate Blend.

Sieve Size		Blend	Control Points, SSPWC*	
No	mm		Lower	Upper
1"	25.00	100.0	100	100
3/4"	19.00	96.3	90	100
1/2"	12.50	83.0		
3/8"	9.50	77.8	63	85
#4	4.75	58.4	45	65
#8	2.36	43.0		
#10	2.00	38.9	30	44
#16	1.180	30.3		
#30	0.600	23.6		
#40	0.425	20.2	12	22
#50	0.300	16.5		
#100	0.150	10.3		
#200	0.075	6.10	3	7

\* Denotes "Standard Specifications for Public Works Construction"

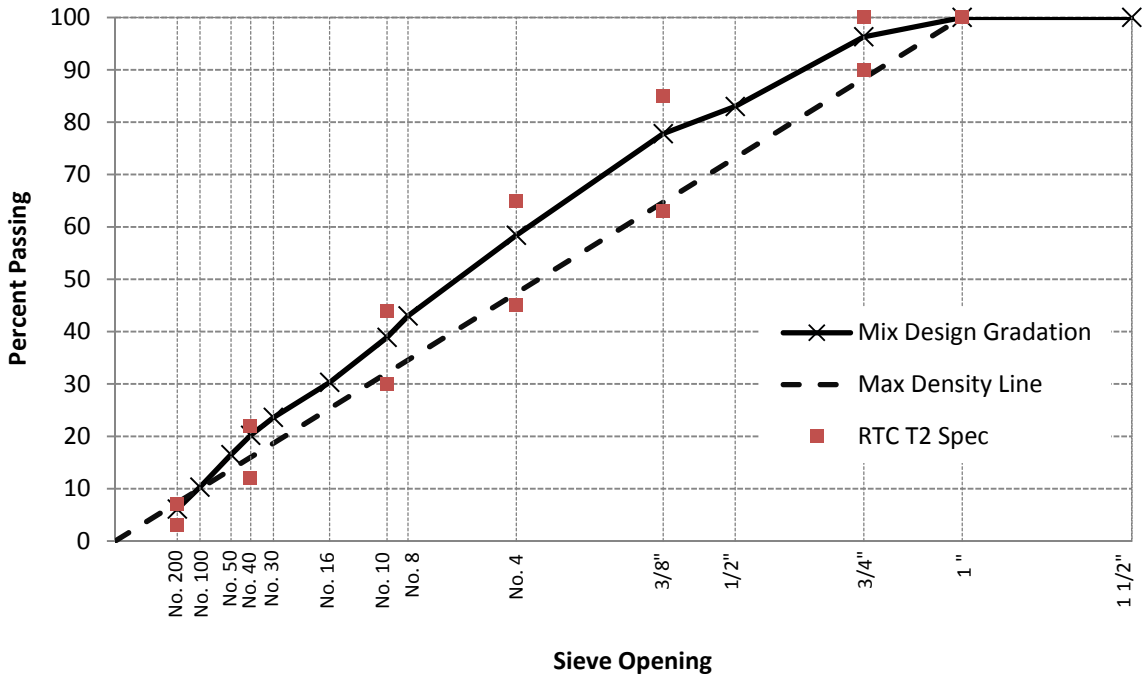


Figure 1. Gradation of the aggregate blend



### 3.2 Asphalt Binders

The PG64-28NV and PG64-28PM asphalt binders were obtained from two sources: Paramount Petroleum and Valero Marketing and Supply. The four asphalt binders were labeled PM-PAR, PM-VAL, NV-PAR and NV-VAL, where PM = PG64-28PM, NV = PG64-28NV, PAR = Paramount and VAL = Valero. Tables 3 and 4 summarize the test results and the PG grading of the various binders.

Table 3. Asphalt Binders Grading Test Results and Specifications.

Test	Spec.	Binder Types				
		PM-PAR	PM-VAL	NV-PAR	NV-VAL	
<b>Tests on Original Binder</b>						
Flash Point, min, °C	230	496	487	391	472	
RV at 135 °C, max, Pas	3.0	0.831	0.929	0.838	0.754	
G*/sin( $\delta$ ) at 64°C, min, kPa	1.00	2.50	2.68	1.85	2.14	
<b>Tests on Residue from RTFOT</b>						
Mass Loss, max, %	1.00	0.419	0.279	0.405	0.166	
G*/sin( $\delta$ ) at 64°C, min, kPa	2.20	5.53	6.05	4.14	3.08	
<b>Tests on Residue from Pressure Aging Vessel @ 100°C</b>						
G* $\sin(\delta)$ at 22°C, max, kPa	5000	2220	1610	1390	2250	
Creep Stiffness at -18°C, max, MPa	300	135	106	114	190	
m-value at -18°C, min	0.300	0.324	0.306	0.324	0.319	
<b>PG Plus Requirement</b>						
<b>Tests on Original Binder</b>						
NDOT	Ductility (5cm/min), cm, at 4°C, min	50.0	<u>15.0*</u>	<u>42.0*</u>	59.0	<u>40.0*</u>
	Toughness (in-lbs) at 25 °C, min	110.0	<u>65.4*</u>	<u>97.1*</u>	130.4	110.8
	Tenacity (in-lbs) at 25 °C, min	75.0	<u>32.7*</u>	<u>67.5*</u>	113.3	86.7
<b>Tests on Residue from RTFOT</b>						
NDOT	Ductility (5cm/min), cm, at 4°C, min	25.0	<u>7.0*</u>	<u>17.0*</u>	35.0	<u>22.0*</u>
Caltrans	$\delta$ when G*/sin( $\delta$ ) = 2.2 kPa, max	80.0	66.1	65.2	65.1	66.5
	Elastic recovery at 25°C, min, %	75.0	87.0	85.0	75.0	80.0

\* Did not meet the NDOT PG-plus specification for PG64-28NV.

Table 4. Binders PG Grading.

Binder Types	True Grade	PG Grade	Meets PG-plus Spec for	
			PG64-28PM	PG64-28NV
PM-PAR	73.3-31.5	70-28	Yes	No
PM-VAL	73.7-29.8	70-28	Yes	No
NV-PAR	70.4-31.5	70-28	Yes	Yes
NV-VAL	67.4-30.2	64-28	Yes	No

The test results show that all binders met the corresponding PG-plus requirements (i.e. PM and NV) except for the PG64-28NV asphalt binder supplied by Valero (i.e. NV-VAL) which failed to meet the ductility requirements for the original and RTFO-aged asphalt binder. The PM-PAR, PM-VAL and NV-VAL asphalt binders met the PM requirements but failed to meet the NV requirements. On the other hand, only the NV-PAR asphalt binder met both PM and NV specifications. Consequently, the NV-VAL asphalt binder was excluded from further evaluation.

### 3.3 Mix Designs

All HMA mixes were designed using the Marshall design method specified by the Washoe County RTC specifications and as outlined in the Asphalt Institute's Mix Design Methods Manual (MS-2). The virgin aggregate samples were mixed with various amounts of asphalt binder so that at least two were above and at least two were below the expected optimum asphalt content. All mixtures were designed with a minimum dry tensile strength of 65 psi at 77°F and minimum retained tensile strength ratio (TSR) of 70%. Hydrated lime was added to the mixtures in the form of dry hydrated lime on wet aggregate (3% moisture above the saturated surface dry condition) at 1.5% by dry weight of aggregate. The samples were compacted with 75 blows on each side with the standard Automated Marshall hammer. The compaction effort is controlled by the expected design ESALs for the project, with 75 blow designs being required on projects over 1 million ESALs.

Three samples were prepared at each of the specified asphalt contents. The measured properties included: Marshall stability and flow, air-voids, voids filled with asphalt binder (VFA), voids in mineral aggregate (VMA) and unit weight. **Figures 2 to 4** present the relationships between the measured properties and binder content.

The optimum binder content was selected at four percent air-voids. The selected binder content was then used to determine the corresponding values for Marshall stability and flow, VMA, and VFA from the appropriate relationships. **Table 5** summarizes the mix design data and the corresponding SSPWC specifications. The optimum asphalt binder contents were 5.0% by total weight of mix for all evaluated mixtures.

The moisture sensitivity of the various mixtures was evaluated using the unconditioned and moisture-conditioned tensile strengths (TS) along with the tensile strength ratio (TSR) after one freeze-thaw (F-T) cycle. The TSR is measured as the ratio of the moisture-conditioned TS over the unconditioned TS of the HMA. The testing followed the procedure outlined in AASHTO T283. For each mixture, a total of ten 4-inch diameter samples were compacted using the Marshall compactor to  $7\pm 0.5\%$  air voids. The samples were divided into two subsets of five samples each: unconditioned subset (i.e. at 0 F-T) and moisture-conditioned subset (i.e. after 1 F-T). The samples from the moisture-conditioned subset were subjected to  $75\pm 5\%$  saturation before being subjected to the freeze-thaw cycle which consisted of freezing the samples at 0°F for 16 hours followed by 24 hours thawing at 140°F and 2 hours at 77°F. **Figure 5** summarizes the test results for the TS and TSR for the three evaluated mixtures with the error bars representing the 95% confidence intervals. Overlapping of the confidence intervals implies the similarity in the measured TS between the mixtures' types. A paired mean comparison analysis at a significance level of 0.05 was conducted to determine whether there is any statistical significant difference between the TS of the various evaluated mixtures.

The data show that all three mixtures met the minimum TS and TSR of 65 psi and 70%, respectively. The PM-PAR mix exhibited significantly higher unconditioned and moisture-conditioned TS values when compared to the PM-VAL and NV-PAR mixes. The PM-VAL and NV-PAR mixes exhibited similar TS values at 77°F. However, a lower TSR was observed for the PM-PAR mix when compared to the other two mixes.

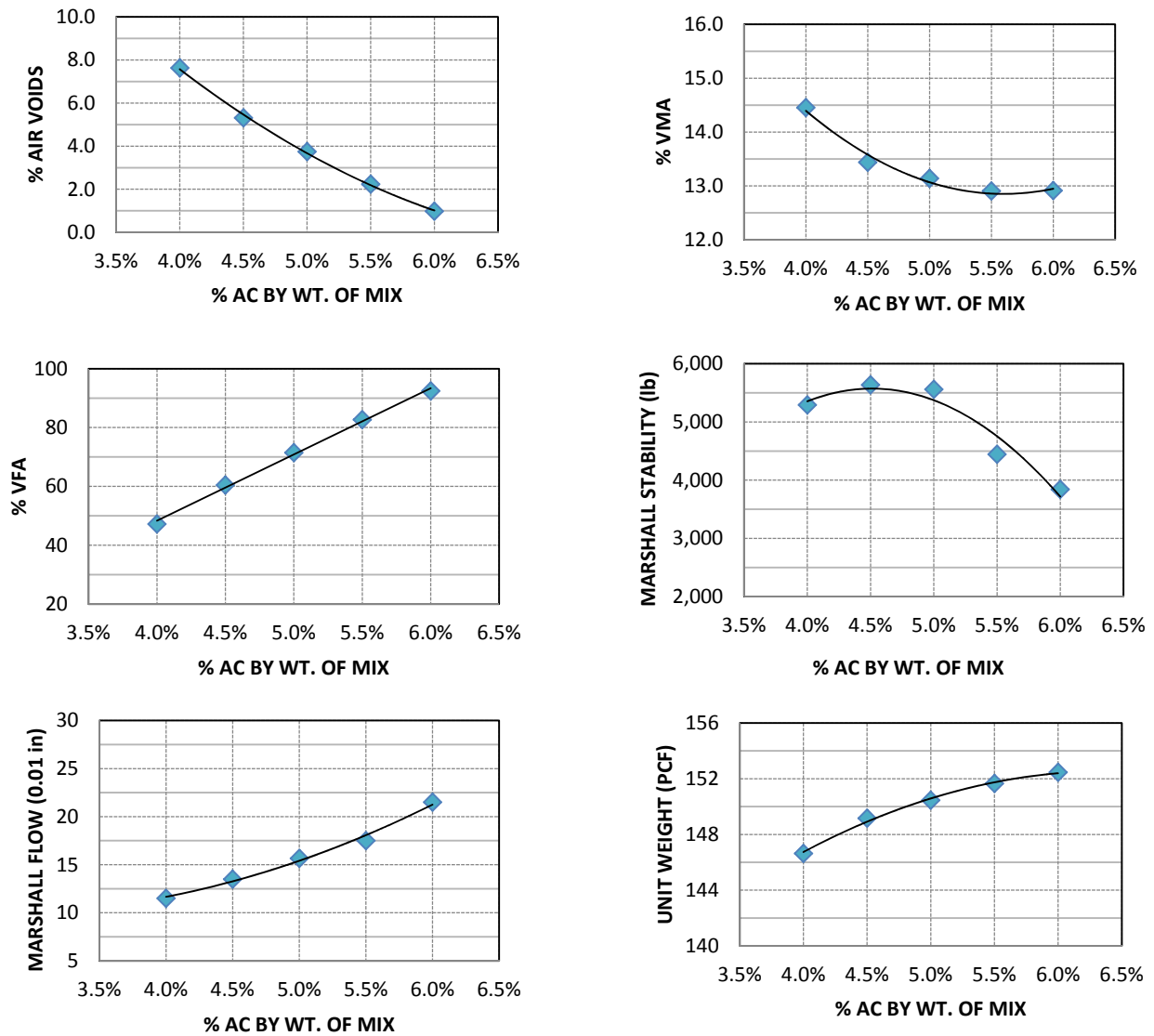


Figure 2. Marshall mix design relationships for PM-PAR

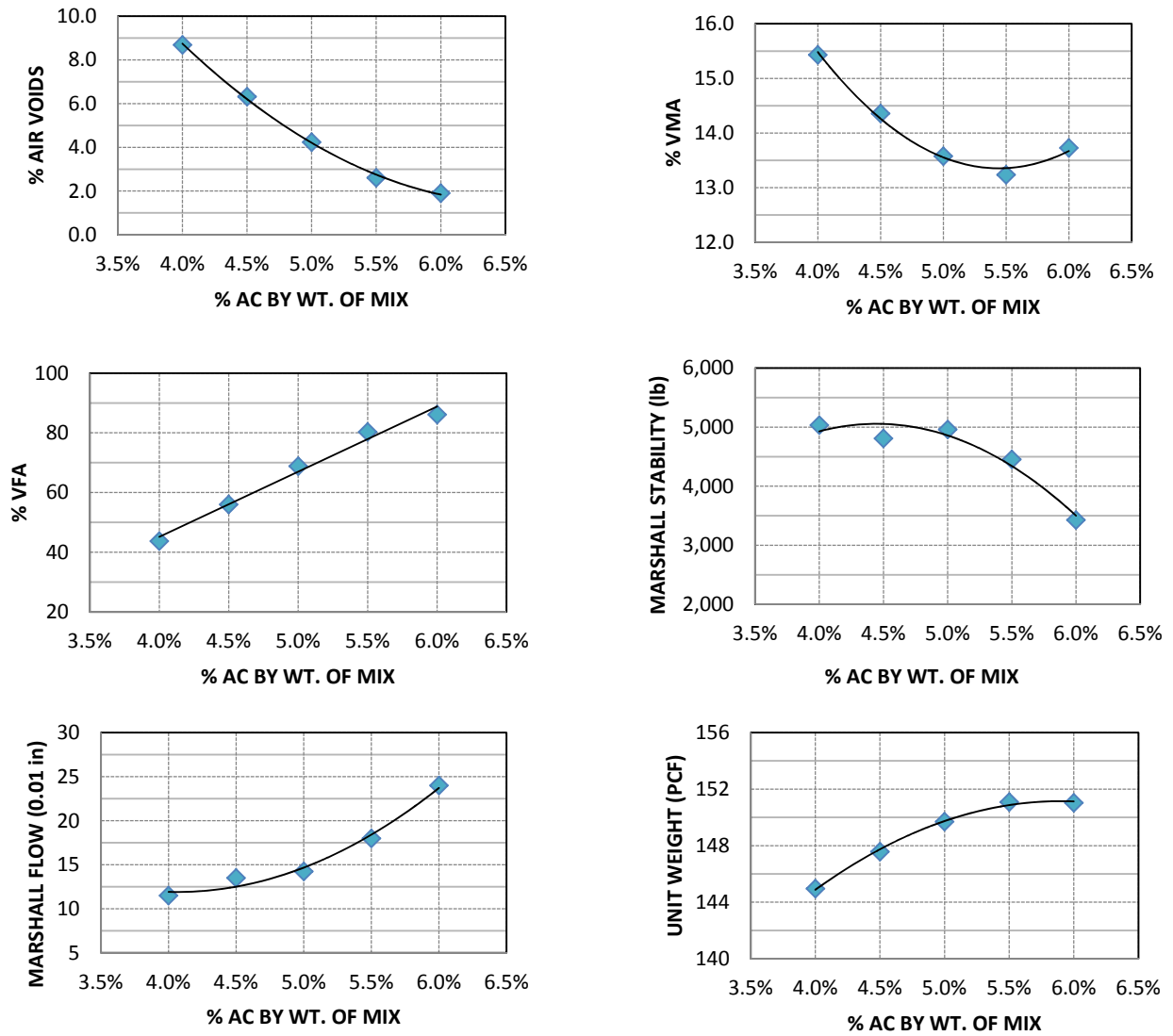


Figure 3. Marshall mix design relationships for PM-VAL

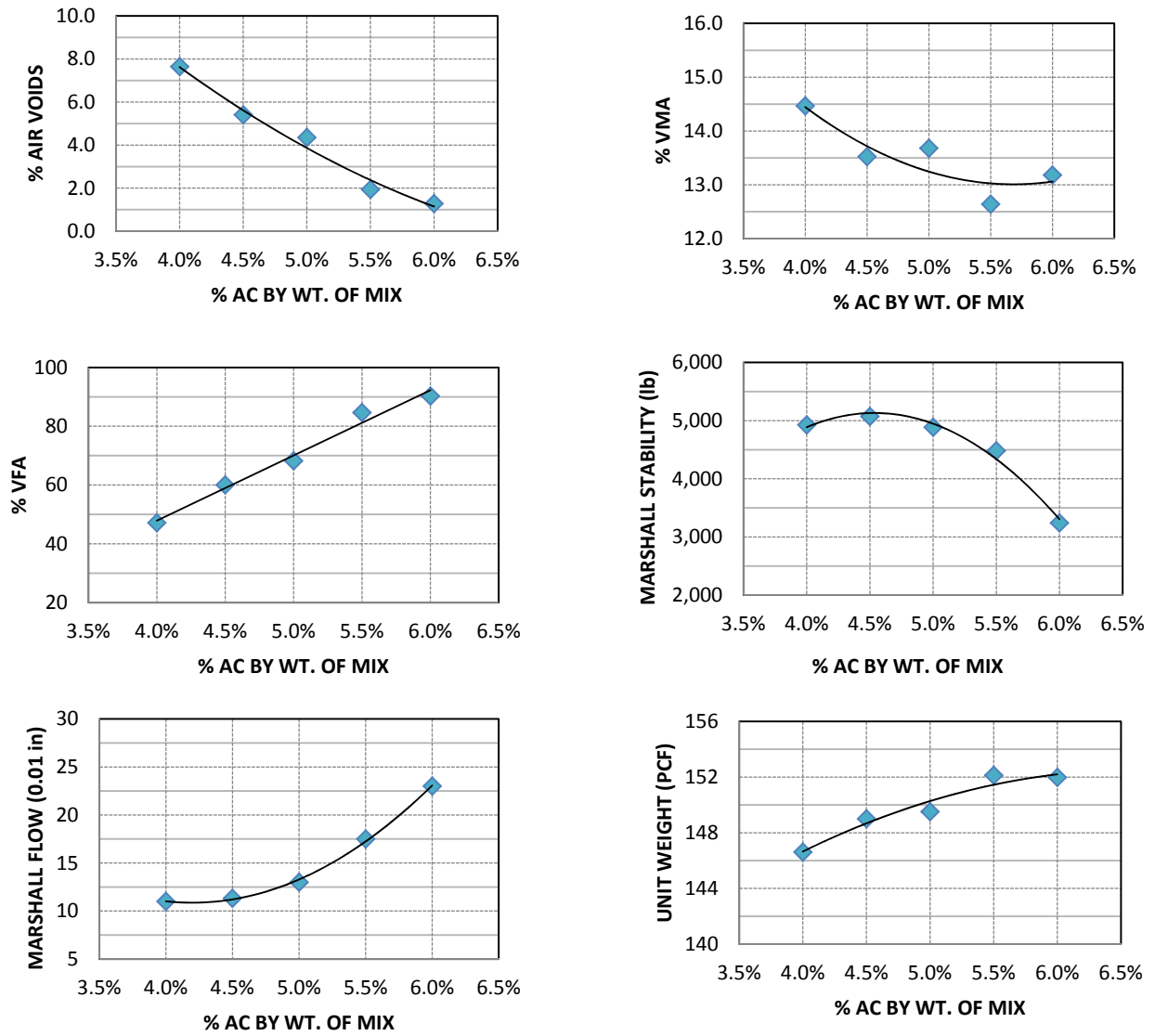


Figure 4. Marshall mix design relationships for NV-PAR

Table 5. Mix Designs Summary and Specifications.

Property	PM-PAR	PM-VAL	NV-PAR	SSPWC Specification
Mixing Temperature Range (°F)	325-328	329-332	335-339	--
Compaction Temperature Range (°F)	315-320	320-324	324-329	--
Optimum Binder Content (%TWM*)	5.0	5.0	5.0	--
Voids in Total Mix (%)	4.0	4.0	4.0	3-5
Voids in Mineral Aggregate, VMA (%)	13.1	13.6	13.3	13 Min.
Voids Filled with Asphalt, VFA (%)	67.4	66.7	69.0	65-75
Marshall Stability (lb)	5347	4844	4988	1800 Min.
Marshall Flow (0.01 inch)	15	14	13	8-20
Maximum Theoretical Specific Gravity	2.505	2.505	2.505	--
Unit Weight (pcf)	150.4	149.6	150.1	--

\* Denotes "Total Weight of Mix"

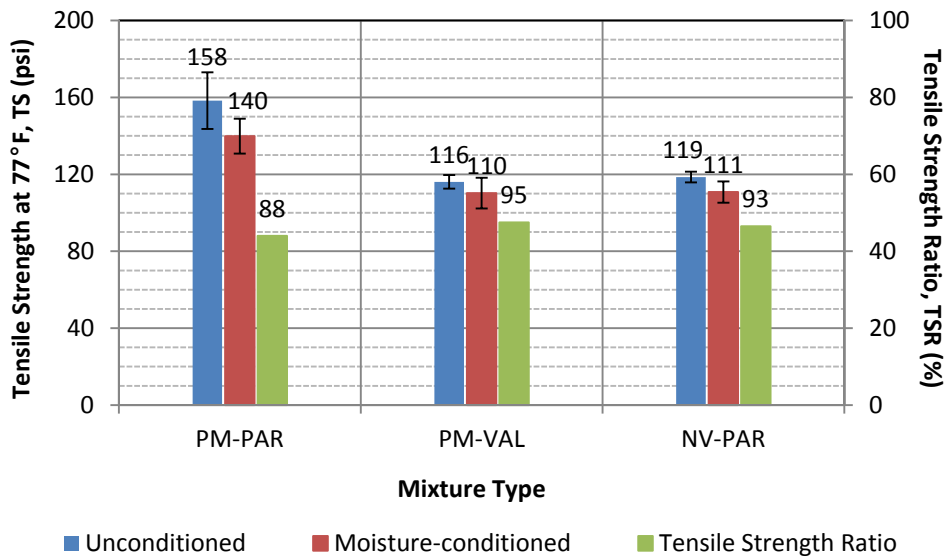


Figure 5. Tensile strength values and ratios at 77°F

(Numbers above bars represent means and whiskers represent mean  $\pm$  95% confidence interval)

#### 4. EXPERIMENTAL PROGRAM

The experimental program for this effort is shown in [Table 6](#). The HMA mixes were evaluated with the most widely accepted laboratory tests for the following modes of pavement failure:

- Moisture damage
- Fatigue cracking
- Permanent deformation
- Thermal cracking

Table 6. Experimental Program.

Properties <sup>s</sup>	Mixture Type (All Lime-Treated)			
	PM-PAR	PM-VAL	NV-PAR	NV-VAL
Resistance to Moisture Damage (short-term aged): • E* vs. F-T cycles: 0, 1 and 6	X	X	X	NT*
Resistance to Permanent Def. (short-term aged): • FN test at 136°F • Rutting characteristic at 136°F	X	X	X	NT
Resistance to Fatigue Cracking (long-term aged): • Flexural beam characteristic at 70°F	X	X	X	NT
Resistance to Thermal Cracking (long-term aged): • TSRST test	X	X	X	NT

<sup>s</sup> F-T denotes freeze-thaw, E\* refer to dynamic modulus, FN denotes flow number and TSRST denotes thermal stress restrained specimen test.

\* NT denotes “Not Tested” because binder failed to meet NDOT PG-plus specification

Some of the properties were evaluated at the unaged stage while others were evaluated at the aged stage. For example, in the case of resistance to permanent deformation, the HMA mixtures were evaluated at the unaged stage because permanent deformation is a short-term distress mode. On the other hand, the fatigue and thermal cracking resistance of the HMA mixtures were evaluated at the aged stage because fatigue and thermal cracking are long-term distress modes. The dynamic moduli, E\*, of the various mixtures were evaluated under the unaged stage. Following the Superpave recommendations for mechanical properties, short-term aging of HMA mixtures consisted of subjecting loose mixtures to 275°F in a forced-draft laboratory oven for 4 hours prior to being compacted. For long-term aging of HMA mixtures, the compacted samples were subjected to a temperature of 185°F for 5 days in a forced-draft laboratory oven, after being short-term aged.

## 5. DESCRIPTION OF LABORATORY TESTS

### 5.1 Moisture Damage Testing

The resistance of the various HMA mixtures to moisture damage was evaluated in terms of measuring the dynamic modulus of the mixtures under multiple freeze-thaw (F-T) cycling. The multiple F-T cycling followed the procedure outlined in AASHTO T-283 at multiple stages. A total of three Superpave gyratory compacted samples from each mix were evaluated following the procedure outlined below. All test specimens were compacted to  $7 \pm 0.5\%$  air voids.

- Measure the unconditioned E\* master curve (i.e., 0 F-T cycles).
- Subject the samples to 70-80% saturation.
- Subject the saturated samples to multiple freeze-thaw cycling wherein one freeze-thaw cycle consists of freezing at 0°F for 16 hours followed by 24 hours thawing at 140°F and 2 hours at 77°F.
- Subject each sample to the required number of freeze-thaw cycles.
- Conduct E\* testing after cycles: 1 and 6.

The AASHTO Mechanistic-Empirical Pavement Design Guide (MEPDG) uses the dynamic modulus ( $E^*$ ) master curve to evaluate the structural response of the HMA pavement under various combinations of traffic loads, speed, and environmental conditions. The  $E^*$  property of the various HMA mixtures is evaluated under various combinations of loading frequency and temperature. The test is conducted at frequencies of: 25, 10, 5, 0.5, 0.1 Hz and at temperatures of: 40, 70, 100, and 130°F. Using the viscoelastic behavior of an HMA mixture (i.e. interchangeability of the effect of loading rate and temperature), the master curve can be used to identify the appropriate  $E^*$  for any combination of pavement temperature and traffic speed. **Figure 6** shows the components and testing conditions of the complex modulus test along with a typical master curve for HMA mixtures.

The  $E^*$  property provides an indication on the general quality of the HMA mixtures. The relationship between  $E^*$  and the number of F-T cycles gives an indication on the moisture resistance of the HMA mixture.

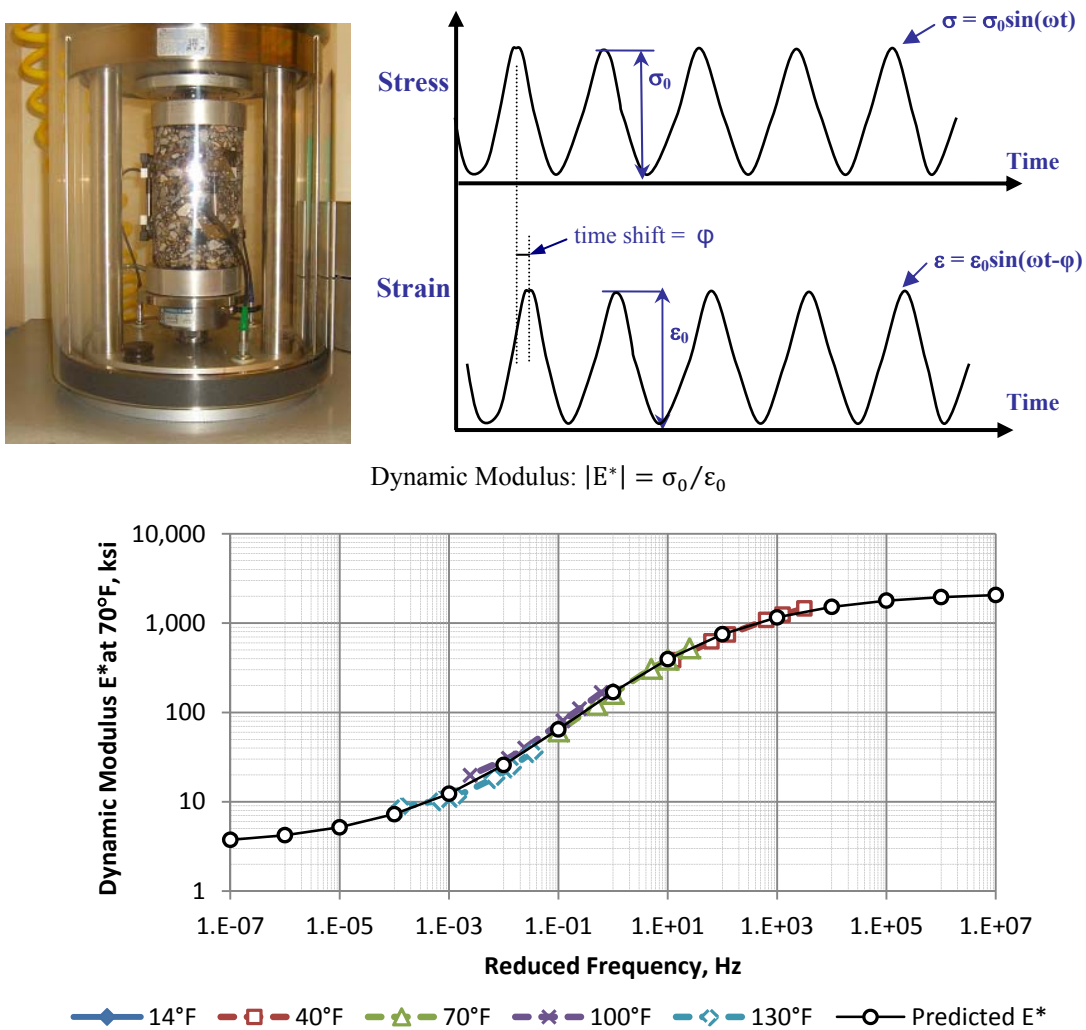


Figure 6. Components of the dynamic modulus test and typical  $E^*$  master curve



## 5.2 Permanent Deformation Testing

The resistance of HMA mixtures to permanent deformation was evaluated using the repeated load triaxial test (RLT). The fundamental test provides engineering properties of the mixtures that can be used in the mechanistic-empirical analyses of HMA pavements containing the various mixtures. The RLT test consists of testing a 4 inch by 6 inch cylindrical sample under triaxial state of stress. The test specimens were cored out of a 6 inch by 7 inch Superpave gyratory compacted sample. All test specimens were compacted to  $7 \pm 0.5\%$  air voids. A repeated haversine deviator stress of 80 psi is applied for 0.05 second followed by a 0.45 second rest period while keeping the surrounding confining pressure constant at 30 psi. All mixes were tested at a temperature of 136°F. Figure 7 shows the components of the RLT test and typical response. The axial deformation of the sample is measured over the middle 4.0 inches of the sample by two linear variable differential transformers (LVDTs) placed 180 degrees apart. The LVDTs measure both the resilient and permanent deformations. The axial permanent strain is calculated as the ratio of the permanent deformation over the 4.0 inches gauge length times 100.

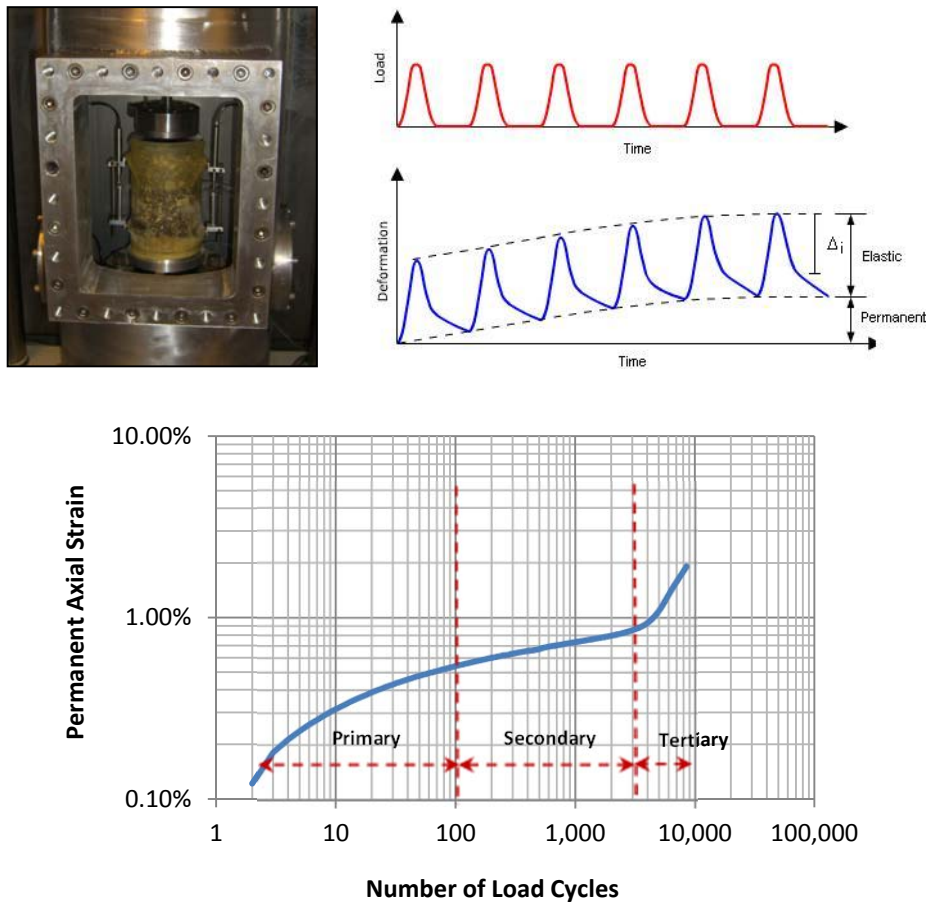


Figure 7. Components of repeated load triaxial test and typical permanent deformation curve

The resulting cumulative permanent axial strain is plotted versus the number of load cycles. The cumulative permanent strain can be defined by the primary, secondary, and tertiary zones (Table 1). In the primary zone, the permanent strain increases rapidly but at a decreasing rate. In the secondary zone, the permanent strain rate maintains a constant value until it starts increasing in

the tertiary creep zone. Only the secondary stage is used to characterize the permanent deformation behavior of the HMA mixtures using the following model:

$$\frac{\varepsilon_p}{\varepsilon_r} = a(N_r)^b \quad (1)$$

where  $\varepsilon_p$  is the permanent axial strain (in/in),  $\varepsilon_r$  is the resilient axial strain (in/in),  $N_r$  is the number of loading repetitions, and  $a$  and  $b$  are experimentally determined coefficients. Equation 1 shows that the lower the  $\varepsilon_p/\varepsilon_r$ , the higher the rutting resistance of the mix.

The point at which the tertiary flow starts (i.e. end of secondary stage) is called the flow number (FN). In other words, the FN is defined as the number of load cycles corresponding to the minimum rate of change of permanent axial strain. The higher the FN value the higher the mixture's resistance to rutting.

### 5.3 Fatigue Cracking Testing

The resistances of the various HMA mixtures to fatigue cracking were evaluated using the flexural beam fatigue test "AASHTO T321-07: Determining the Fatigue Life of Compacted Hot-Mix Asphalt Subjected to Repeated Flexural Bending". A 2.5×2.0×15 inches beam specimen is subjected to a 4-point bending with free rotation and horizontal translation at all load and reaction points. This produces a constant bending moment over the center portion of the specimen. All beams were compacted using the kneading compactor to  $7 \pm 0.5\%$  air voids. In this research, constant strain tests were conducted at different strain levels; using a repeated sinusoidal load at a frequency of 10 Hz, and a test temperature of 70°F. The initial flexural stiffness was measured at the 50<sup>th</sup> load cycle. Fatigue life or failure was defined as the number of cycles corresponding to a 50% reduction in the initial stiffness. The following model was used to characterize the fatigue behavior of the HMA mixtures:

$$N_f = k_1 \left( \frac{1}{\varepsilon_f} \right)^{k_2} \quad (2)$$

where  $N_f$  is the fatigue life (number of load repetitions to fatigue damage),  $\varepsilon_f$  is the applied tensile strain in in/in, and  $k_1$  and  $k_2$ , are experimentally determined coefficients. **Figure 8** shows the schematics of flexural beam fatigue and typical fatigue curve for HMA mixtures. All the fatigue samples were long-term aged following the Superpave recommendation for long-term aging of HMA mixtures which consists of subjecting the compacted samples to 185°F temperatures for 5 days in a forced-draft laboratory oven.

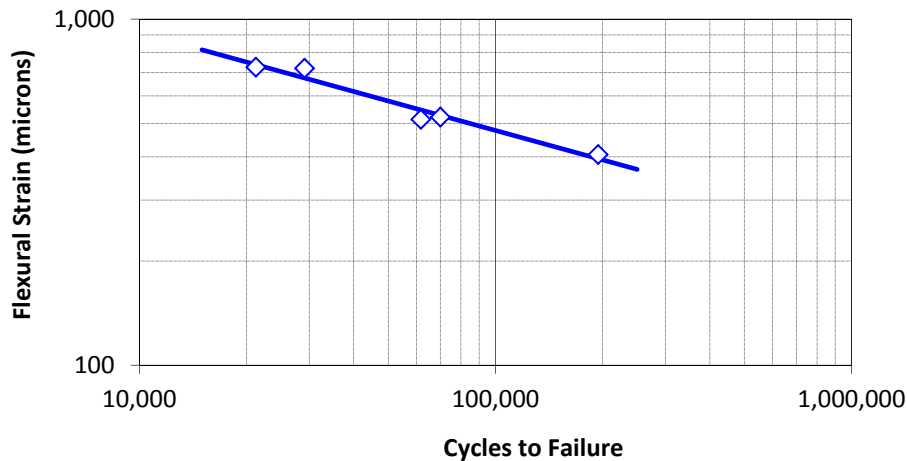


Figure 8. Components of beam fatigue test and typical fatigue curve at a given temperature

#### 5.4 Thermal Cracking Testing

The Thermal Stress Restrained Specimen Test (TSRST) was used to determine the low-temperature cracking resistance of the various HMA mixtures. The test cools down a cylindrical specimen at a rate of 10°C/hour. While the specimen is being cooled down, tensile stresses are generated due to the ends being restrained. The HMA mixture would fracture as the internally generated stress exceeds its tensile strength. The temperature and stress at which fracture occurs is referred to as “fracture temperature” and “fracture stress”, respectively, and represents the field temperature under which the pavement will experience thermal cracking. [Table 1](#) shows the schematics of the TSRST and a typical stress versus temperature relationship for HMA mixtures. Two test specimens of 2.25 inch diameter by 5.5 inch high were cored sideways from a 4 inch diameter by 6 inch high Superpave gyratory compacted sample. Specimens’ air voids were maintained within  $7 \pm 0.5\%$ . All the TSRST samples were long-term aged following the Superpave recommendation for long-term aging of HMA mixtures which consisted of subjecting the compacted samples to 185°F temperature for 5 days in a forced-draft laboratory oven before coring out the test specimens.

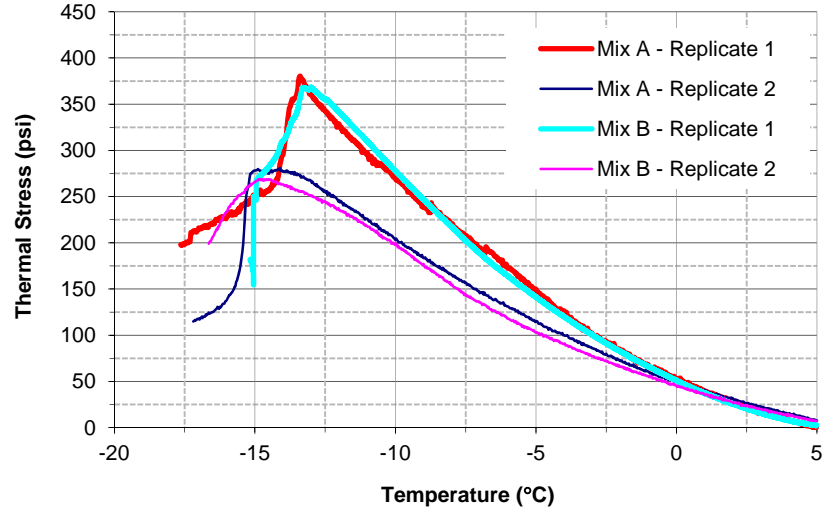


Figure 9. Components of TSRST test and typical stress-temperature curves for HMA mixes

## 6. ANALYSIS OF LABORATORY TEST RESULTS

This section of the report presents the test results and the analysis of the data that were generated from the various laboratory evaluations of the three HMA mixtures. As mentioned earlier, the mixture with Valero PG64-28NV asphalt binder was not evaluated due to the fact that it did not meet NDOT specification for NV binders.

### 6.1 Resistance of the HMA Mixtures to Moisture Damage

The resistance of the various HMA mixtures to moisture damage was evaluated in terms of measuring the dynamic modulus master curves of short-term aged mixtures after multiple F-T cycling. The multiple F-T cycling follows the procedure outlined in AASHTO T-283 at multiple stages and as described previously. For every mixture, the dynamic modulus master curve was measured at the unconditioned stage and after 1 and 6 F-T cycles.

Figures 10 – 12 present the  $E^*$  master curves after 0, 1, and 6 F-T cycles. The PM-PAR mixture (Figure 10) shows the lowest drop while the PM-VAL (Figure 11) shows the largest drop in  $E^*$  master curve as a function of multiple F-T cycling. Figure 13 presents the  $E^*$  property at 70°F and 10 Hz loading of the various mixtures as a function of multiple F-T cycling. The 70°F was selected since it represents a mid-range pavement temperature for the Truckee Meadows region and the 10 Hz loading represents normal traffic speed on major arterials. Figure 13 shows all three mixtures exhibiting reductions in the  $E^*$  property as a function of F-T cycles. However, all three mixtures maintained  $E^*$  property above 400 ksi after 6 F-T cycles which is considered an excellent retained level of stiffness for HMA mixtures.

Figure 14 presents the ratios of the  $E^*$  property after 1 and 6 F-T cycles over the unconditioned  $E^*$  property of the three mixtures. The data in Figure 14 indicate that all three mixtures retained similar percentage of their unconditioned  $E^*$  after 1 F-T while their retained ratios after 6 F-T cycles are significantly different.

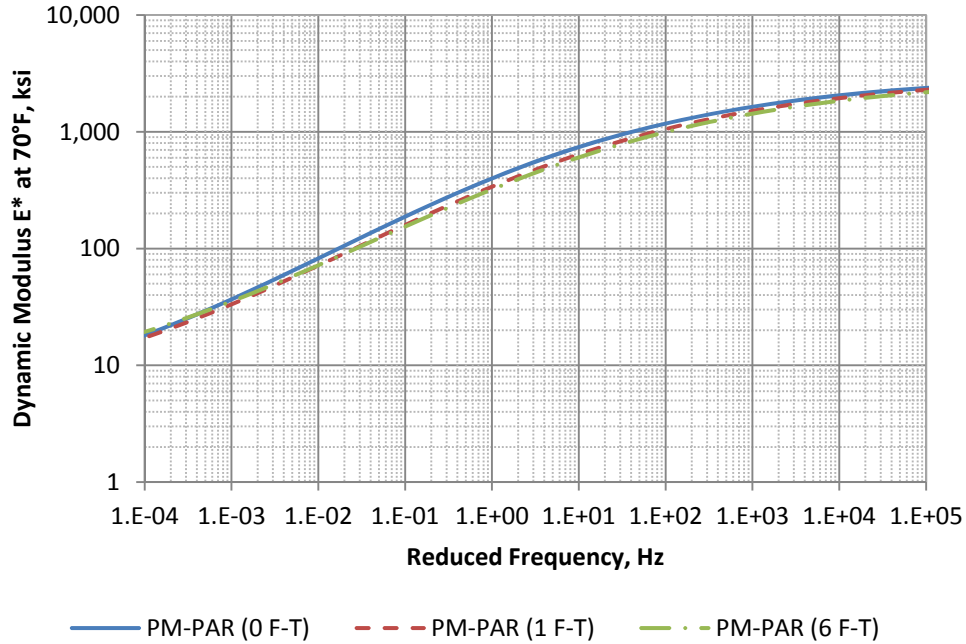


Figure 10.  $E^*$  at multiple F-T cycles for the Paramount PG64-28PM mixture (PM-PAR)

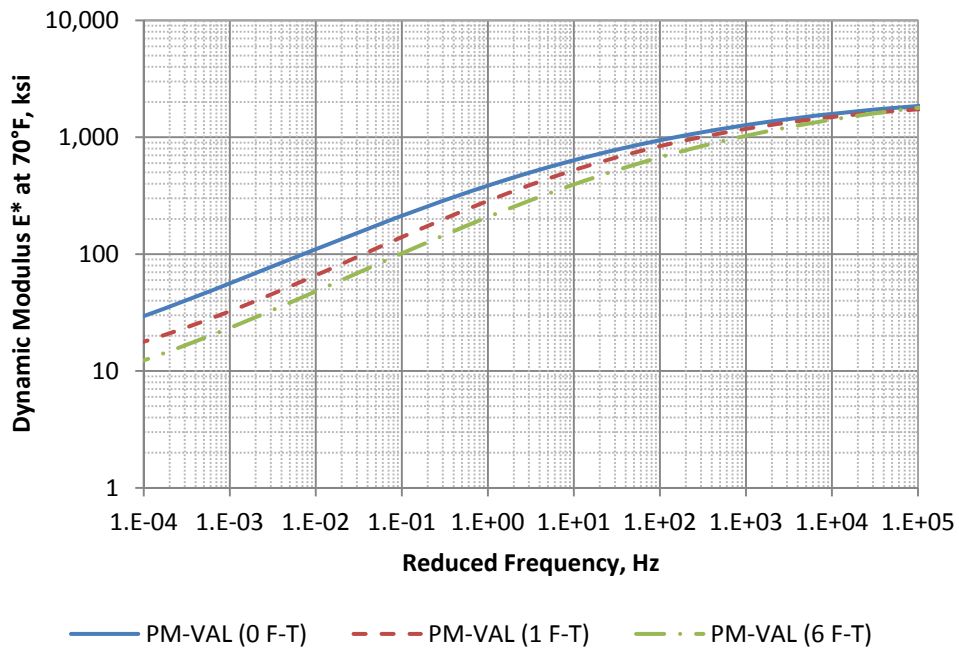


Figure 11.  $E^*$  at multiple F-T cycles for the Valero PG64-28PM mixture (PM-VAL)

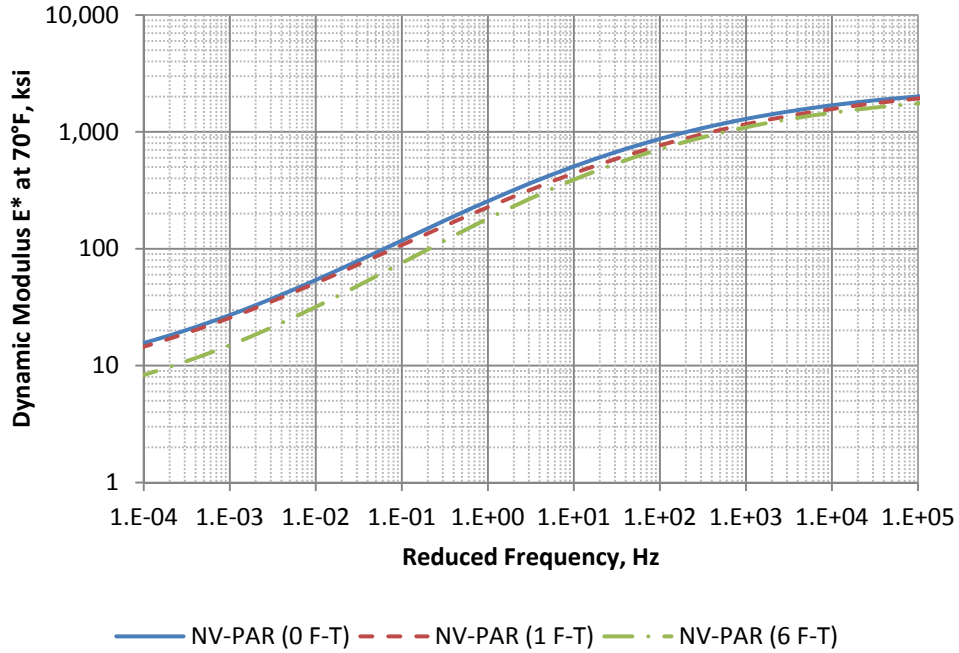


Figure 12. E\* at multiple F-T cycles for the Paramount PG64-28NV mixture (NV-PAR)

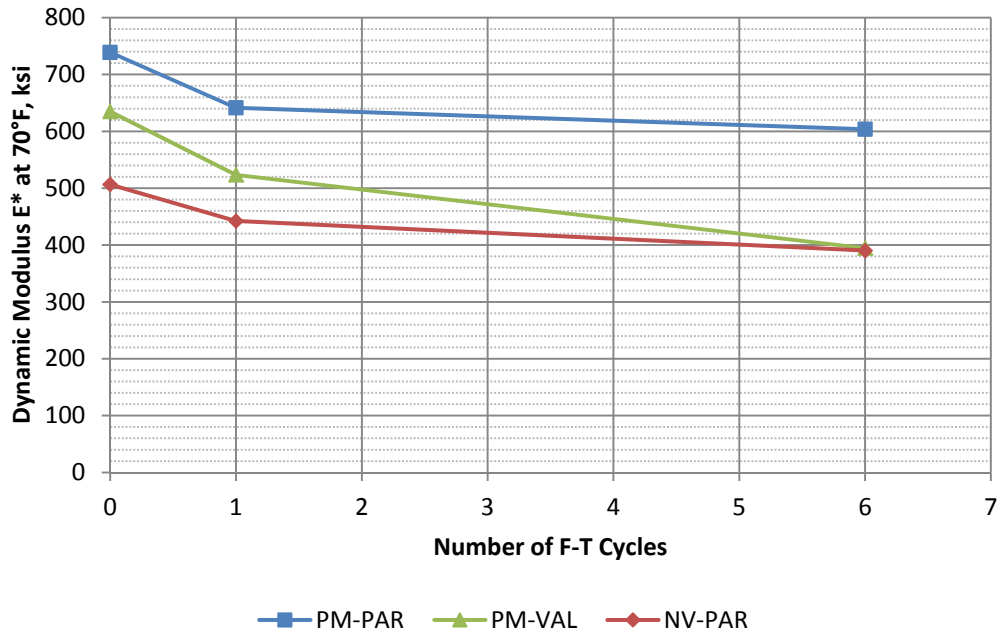


Figure 13. Dynamic Modulus E\* at 10 Hz and 70°F as a function of freeze-thaw cycles

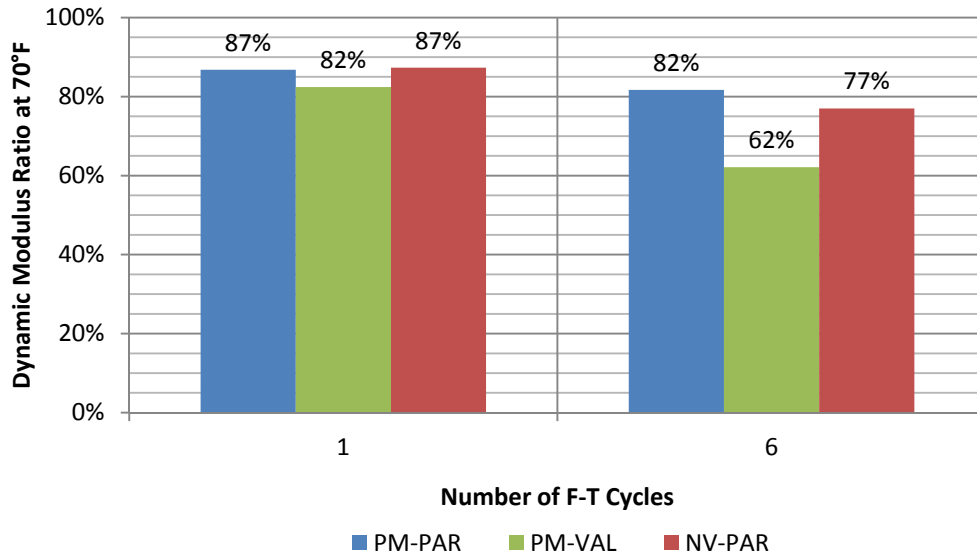


Figure 14. Dynamic Modulus Ratio of the various mixtures at 1 and 6 F-T cycles

Combining the information presented in Figures 10 – 14, it can be concluded that:

- The PM-PAR mix has the highest  $E^*$  property with insignificant percent reduction as a function of multiple F-T cycles.
- The NV-PAR mix has the lowest  $E^*$  property with insignificant percent reduction as a function of multiple F-T cycles.
- The PM-VAL mix has an intermediate  $E^*$  property with significant percent reduction as a function of multiple F-T cycles.

## 6.2 Resistance to Permanent Deformation

Figure 15 presents the Flow Numbers for the three mixtures. As defined earlier, the FN represents the number of load cycles to the beginning of the tertiary flow. Examining the data in Figure 15 lead to the following conclusions:

- The FNs of the PM-PAR and PM-VAL mixtures are statistically similar.
- The FNs of the PM-VAL and NV-PAR mixtures are statistically similar.
- The FN of the NV-PAR mix is significantly higher than the FN of the PM-PAR mix.

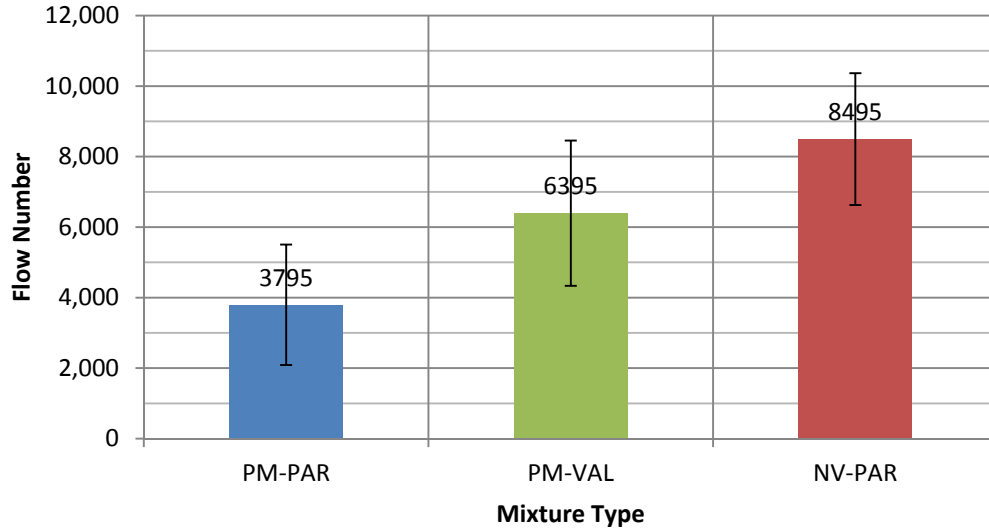


Figure 15. Flow number test results at 136°F for the various mixtures  
(Numbers above bars represent means and whiskers represent mean  $\pm$  95% confidence interval)

Figure 16 shows the permanent deformation models for the three mixtures and Table 7 summarizes the actual statistical models. It should be noted that the higher the curve, the lower the resistance of the mixture to secondary stage permanent deformation. The data in Figure 16 indicate that PM-VAL mix has the best resistance to secondary stage permanent deformation followed by the NV-PAR mix while the PM-PAR mix exhibits the worst. The data also show that the slope of the PM-VAL is much higher than the slope NV-PAR mix (Table 7: 0.554 vs. 0.347) which indicates that the long-term rutting of the PM-VAL mix maybe higher than that of the NV-PAR mix.

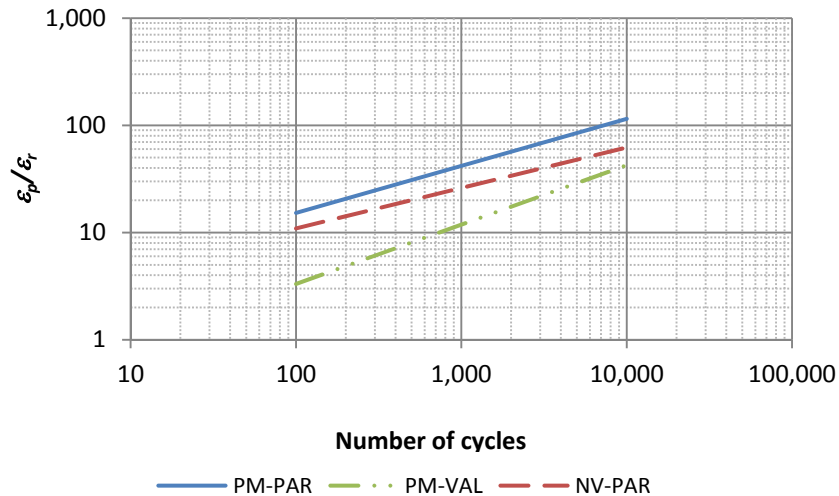


Figure 16. Permanent deformation at 136°F for the various mixtures



Table 7. Permanent Deformation Models at 136°F.

Mix	Rutting Model*
PM-PAR	$\frac{\epsilon_p}{\epsilon_r} = 3.232N^{0.351}$
PM-VAL	$\frac{\epsilon_p}{\epsilon_r} = 0.258N^{0.554}$
NV-PAR	$\frac{\epsilon_p}{\epsilon_r} = 2.454N^{0.347}$

\*  $\epsilon_p$  is the permanent axial strain in in/in,  $\epsilon_r$  is the resilient axial strain in in/in, and  $N_r$  is the number of loading repetitions

### 6.3 Resistance of the HMA Mixtures to Fatigue

The resistances of the various HMA mixtures to fatigue cracking were evaluated using the flexural beam fatigue test at 70°F representing an intermediate weather where fatigue cracking is expected to be a problem. Figure 17 summarizes the fatigue characteristics of the various mixtures in terms of the relationship between the flexural strain and the number of load repetitions to failure. The beam fatigue data were used to develop the fatigue model for each mixture as presented in Equation 2. Table 8 summarizes the fatigue models for all three evaluated mixtures.

Figure 17 shows that all three mixtures had similar number of cycles to fatigue failure at the high strain level (i.e. 700 – 800 microns). As the strain level decreases, the difference among the mixtures becomes more apparent. The NV-PAR mix exhibited a higher number of cycles to failure than both the PM-PAR and the PM-VAL mixtures. The PM-VAL mix showed a better resistance to fatigue cracking than the PM-PAR mix. In summary, the use of PG64-28PM asphalt binders reduced the mixtures' laboratory fatigue resistance when compared to the mixture manufactured with the PG64-28NV binder (i.e. NV-PAR).

Table 8. Fatigue Models at 70°F.

Mix	Fatigue Model*	R <sup>2</sup>
PM-PAR	$N_f = 1.367 \times 10^{-5} \left(\frac{1}{\epsilon}\right)^{2.852}$	0.956
PM-VAL	$N_f = 8.016 \times 10^{-11} \left(\frac{1}{\epsilon}\right)^{4.573}$	0.851
NV-PAR	$N_f = 6.878 \times 10^{-22} \left(\frac{1}{\epsilon}\right)^{8.134}$	0.899

\*  $N_f$  is the fatigue life,  $\epsilon_f$  is the tensile strain in in/in

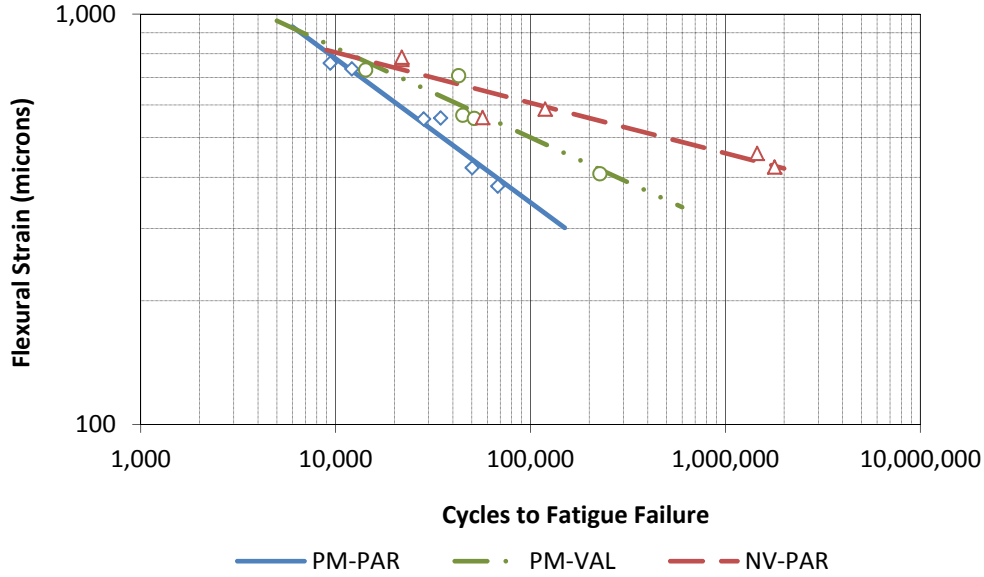


Figure 17. Flexural beam fatigue relationships at 70°F for the various HMA mixes

#### 6.4 Resistance of the HMA Mixtures to Thermal Cracking

The resistances of the mixtures to thermal cracking were measured using the Thermal Stress Restrained Specimen Test (TSRST). The TSRST measures the fracture temperature and fracture stress of HMA mixtures. The fracture temperature represents the temperature at which the HMA mix will develop a transverse crack due to thermal stresses and the fracture stress controls the spacing of the thermal cracks if they occur. It is anticipated that a higher fracture stress in the TSRST would indicate a longer spacing of the transverse cracks in the field. Two cylindrical specimens for each HMA mix were tested and the average results for fracture strength and fracture temperature are presented in Figure 18.

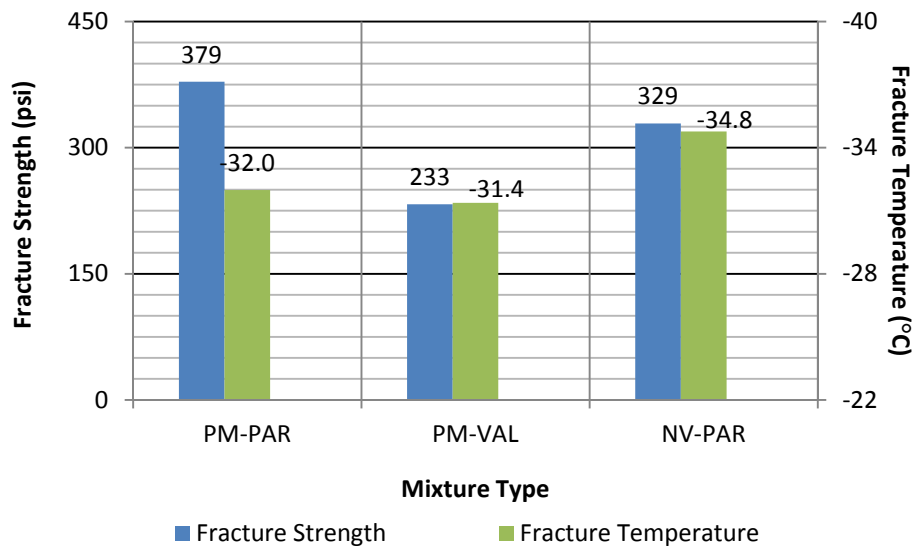


Figure 18. Thermal cracking characteristics of the various mixtures (Numbers above bars represent mean)

The TSRST fracture temperatures data presented in Figure 18 indicate that all three mixtures exceed the expected low pavement temperature for the Truckee Meadows of -28°C. However, the NV-PAR mix will resist lower temperatures than the PM-PAR and PM-VAL mixtures. In the case of fracture stresses, the PM-VAL mix exhibits the lowest while the PM-PAR exhibits the highest. The combination of the lowest fracture temperature and intermediate level of fracture stress for the NV-PAR mix makes it the most resistant to the thermal cracking among the three evaluated mixtures.

## 7.0 MECHANISTIC-EMPIRICAL ANALYSIS

When assessing the impact of mixtures characteristics on the performance of HMA pavements the following two phenomena must be clearly understood:

- In the case of fatigue: the higher the fatigue curve the higher the resistance of the mix to fatigue cracking but the higher the resistance of the mix to fatigue cracking does not necessarily lead to better fatigue performance of the HMA pavement.
- In the case of rutting: the lower the permanent deformation curve the higher the resistance of the mix to rutting but the higher the resistance of the mix to rutting does not necessarily lead to better rutting performance of the HMA pavement.

The above two phenomena may seem to be self-contradicting because of the interaction among the  $E^*$  property of the mix and the fatigue/rutting curves of the HMA mix. For example, in a given HMA pavement structure, the magnitude of the  $E^*$  property controls the magnitude of the generated tensile strain at the bottom of the HMA layer and the vertical strain within the layer which are then used in the fatigue/rutting curves of the HMA mix to estimate the fatigue/rutting performance of the HMA pavement. Therefore, an HMA mix with a higher fatigue/lower rutting curve may still produce a lower estimated fatigue/rutting life of the HMA pavement if its  $E^*$  property is low enough to generate a significantly higher tensile strain at the bottom of the HMA layer or higher vertical strain within the layer.

Based on the above discussion, the rutting and fatigue curves can only be evaluated in terms of the impact of the asphalt binder type on the resistance of the HMA mixtures to fatigue/rutting but not in terms of their impact on the fatigue/rutting performance of the HMA pavement. The impact of the binder on the fatigue/rutting performance of the HMA pavement can only be evaluated through a mechanistic analysis which combines the contributions of both the  $E^*$  property and the fatigue/rutting characteristics of the HMA mix.

The impact of mixture type on the performance of HMA pavements was evaluated through a simplified mechanistic-empirical (ME) analysis of a typical asphalt pavement. The analyses used the unconditioned (i.e. 0 F-T)  $E^*$  properties of the various mixtures to evaluate the response parameters of asphalt pavements that are considered critical to fatigue and rutting of the HMA layer. The following pavement structures were analyzed.

- Asphalt layer: 6 inch thick, modulus varies depending on the type of mix used (see [Table 9](#)).
- Crushed aggregate base layer: 8 inch thick, modulus = 20,000 psi.
- Subgrade layer: infinite, modulus = 8,000 psi.

The loading consisted of a single axle load of 18-kips with dual tires at an inflation pressure of 120 psi. The  $E^*$  values for the various mixtures were obtained from the developed dynamic modulus master curves for a loading frequency of 10 Hz. The  $E^*$  properties at 70°F and 136°F were used for fatigue and rutting analysis, respectively. The temperatures of the  $E^*$  were selected to represent the critical conditions for fatigue cracking of intermediate temperature and permanent deformation of high temperature. Using the three types of asphalt mixtures resulted in six different pavement structures that were analyzed.

The AASHTO MEPDG relates the permanent deformation of the HMA layer to the vertical compressive strain at the middle of the layer and the bottom-up fatigue cracking to the tensile strain at the bottom of the layer. The properties of the pavement structures along with the loading conditions were used in the multi-layer elastic solution to calculate the maximum vertical compressive strain ( $\epsilon_v$ ) at the middle of the HMA layer and the maximum tensile strain ( $\epsilon_t$ ) at the bottom of the layer for all six pavements. The calculated strains are then input into the developed performance models (Equations 1 and 2) of the HMA layer to estimate the rutting and fatigue performance of the HMA pavements.

Table 9. Dynamic Modulus of Various Mixes at 10Hz.

Mix	E* at 10Hz, (ksi)	
	at 70°F	at 136°F
PM-PAR	739	61
PM-VAL	614	80
NV-PAR	486	50

In the case of permanent deformation, it was assumed that all rutting would come from the HMA layer and a rut depth criterion of 0.5 inch was selected. The number of load repetitions to reach the 0.5 inch rutting was estimated from Equation 1 using the appropriate rutting model from [Table 7](#) and the calculated vertical compressive strain ( $\epsilon_v$ ) at the middle of the HMA layer. In the case of fatigue, the number of load repetitions to failure was estimated from Equation 2 using the calculated tensile strain ( $\epsilon_t$ ) at the bottom of the HMA layer and the appropriate fatigue model from [Table 8](#). The number of load repetitions to rutting and fatigue were calculated for the various mixtures and are summarized in [Table 10](#). Examining the data in [Table 10](#) leads to the following observations: the results of the mechanistic-empirical analyses indicated that the rutting and fatigue performance of the two PM pavements are significantly different from each other. On the other hand the rutting performance of the NV pavement falls in-between the two PM pavements while the fatigue performance of the NV pavement is significantly higher than the two PM pavements.

Table 10. Results of the Mechanistic-Empirical Analysis.

Mix	Rutting Analysis at 136°F		Fatigue Analysis at 70°F	
	Maximum vertical compressive strain in the middle of the HMA layer, $\epsilon_r$ (microstrain)	Number of load repetitions ( $N_r$ ) to 0.5" rut depth*	Maximum tensile strain at the bottom of HMA layer, $\epsilon_t$ (microstrain)	Number of load repetitions ( $N_f$ ) to fatigue failure*
PM-PAR	1,109	7,855	207	439,158
PM-VAL	821	48,290	236	3,094,790
NV-PAR	1,383	10,035	277	59,474,627

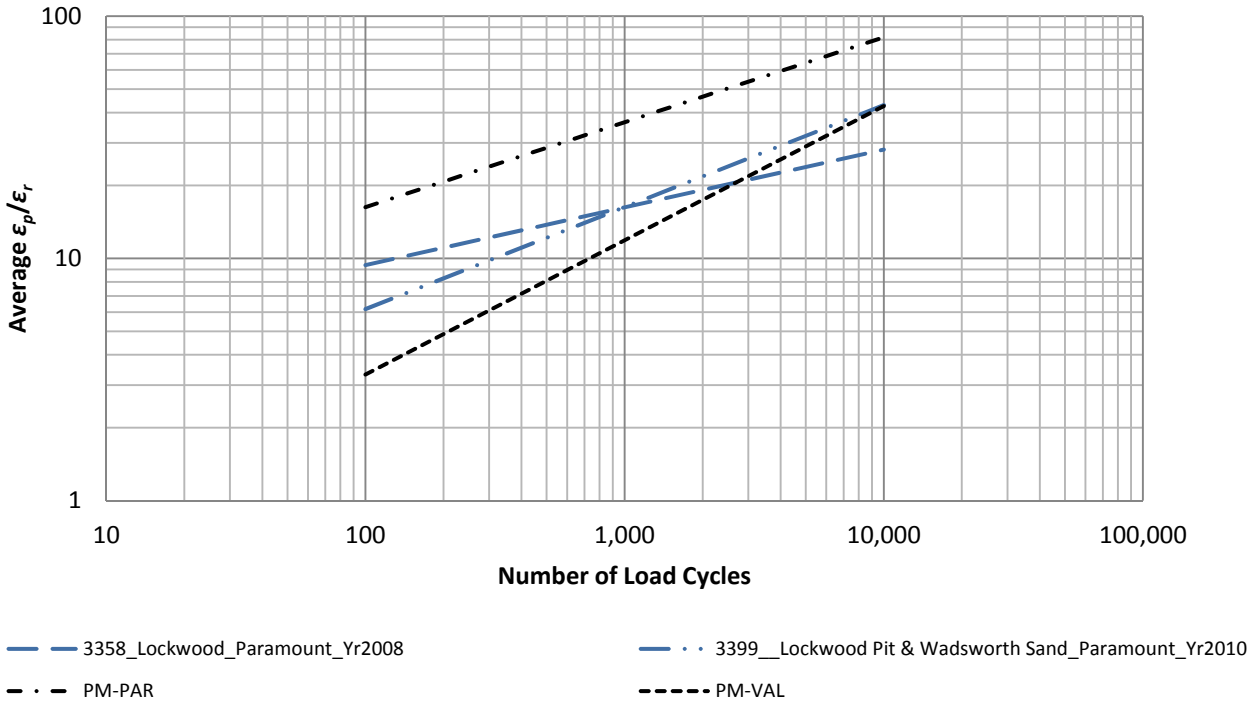
\*  $N_r$  and  $N_f$  were calculated using  $\frac{\epsilon_p}{\epsilon_r} = aN^b$  and  $N_f = k_1 \left(\frac{1}{\epsilon_t}\right)^{k_2}$  equations, respectively.

## 8. CONCLUSIONS

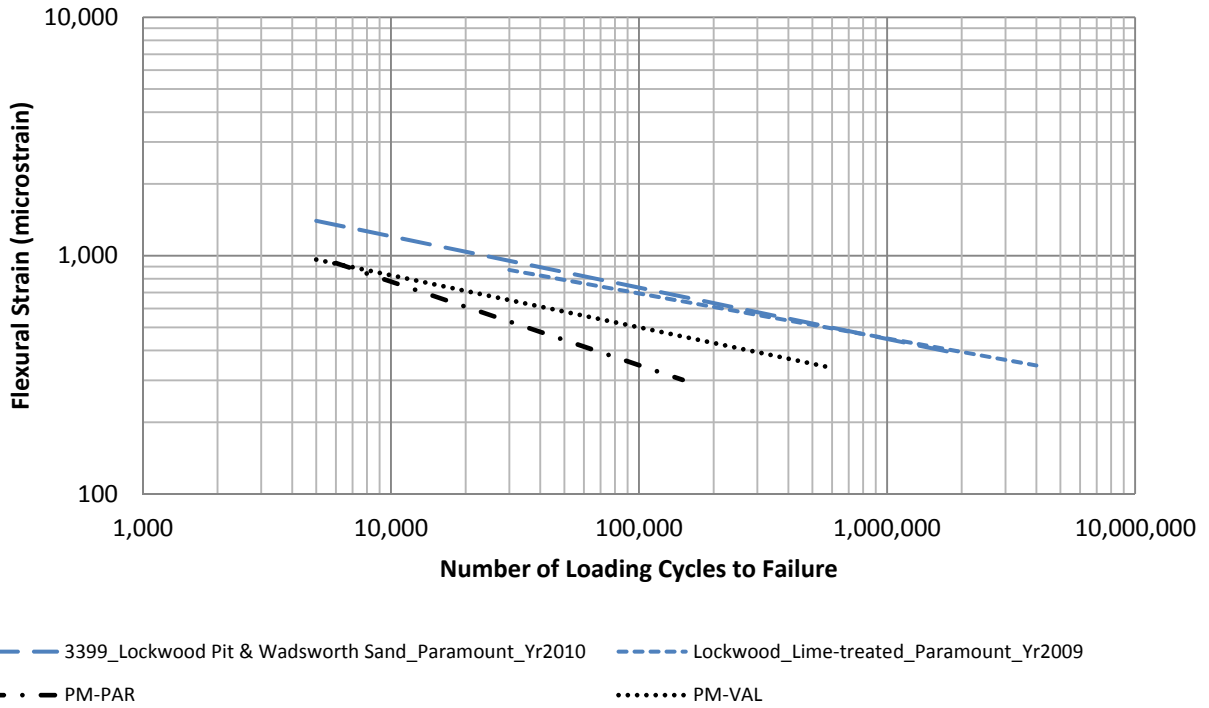
The analyses of the data generated from this laboratory evaluation of PM and NV HMA mixtures and the predicted performance of HMA pavements constructed with the two types of mixtures leads to the following conclusions:

- Both PM mixtures exhibited excellent resistance to moisture damage which is comparable to that of the NV mix. Even-though the  $E^*$  ratio of the PM-VAL mix after 6 F-T is below 70%, the actual value of the  $E^*$  at 70°F after 6 F-T is around 400 ksi which is an excellent level of stiffness.
- The resistances of the two PM mixtures to permanent deformation are significantly different from each other while the resistance of the NV mix to permanent deformation falls between the two PM mixtures. Even-though the PM-VAL mix showed a lower permanent deformation curve than the NV-PAR mix, the significantly lower slope of the NV-PAR mix represents a more stable mix under repeated loading.
- The resistances of the two PM mixtures to fatigue cracking are significantly different from each other and both have significantly lower resistance to fatigue cracking than the NV mix.
- The resistances of the two PM mixtures to thermal cracking are slightly lower than the resistance of the NV mix to thermal cracking. However, both types of mixtures are expected to perform well in terms of resisting thermal cracking in the Truckee Meadows area.
- In terms of the overall performance of HMA pavements, the PM pavements rutting performance is similar to the NV mix while their fatigue performance is significantly lower than that of the NV pavement.
- In general, the behavior and performance of the two PM mixtures that were evaluated in this study were significantly different from each other in many aspects of HMA pavements. Based on these observations it may be concluded that at this point, the PM mixtures may not be consistent enough to be accepted in place of NV mixtures in HMA pavements constructed in the Truckee Meadows area. In order to further examine this

issue, the behavior of two NV mixtures in the RLT and the beam fatigue tests were compared to the behavior of the two PM mixtures as shown in **Figure 19**. The NV mixtures were selected to have the same aggregate source (Lockwood) and the same gradation (NDOT type 2C). The two PM mixtures also have the same aggregate source (Lockwood) and the same gradation (RTC Type 2). The data presented in **Figure 19** should not be used to compare the absolute performance of the NV mixtures with the PM mixtures since the two mixtures have significantly different gradations and different mix design methods (Type 2-Marshall vs. Type 2C-Hveem). However, the data in **Figure 19** can be used to compare the variations in the behavior of the NV and PM mixtures when each binder is used with a constant aggregate source, gradation and mix design method. The data in **Figure 19** clearly show that the PM mixtures are significantly more variable than the NV mixtures in both the RLT and beam fatigue testing. This further supports the observations that were made concerning the high variability of the PM mixtures.



(a)



(b)

Figure 19. Comparison of the variations in the behavior of NV and PM mixtures (a) RLT at 58°C and (b) flexural beam fatigue at 70°F

## **9.0 REFERENCES**

American Association of State Highway and Transportation Officials (AASHTO). Standard Specifications for Transportation Materials and Methods of Sampling and Testing. 29<sup>th</sup> Edition, Washington, D.C., 2009.

National Cooperative Highway Research Program (NCHRP). Guide for Mechanistic-Empirical Design of New and Rehabilitated Structures. Final Report for Project 1-37A, Transportation Research Board, National Research Council, Washington, DC, 2004.

Orange Book, Standard Specifications for Public Works Construction, Regional Transportation Commission (RTC) of Washoe County, 2007.